Transition-Metal-Substituted Alanes: Synthesis and Spectroscopic Studies and the Structure of $(\eta^5\text{-}C_5H_5)(CO)_2Fe{-}Al[(CH_2)_3NMe_2]({}^iBu)$†

Roland A. Fischer* and Thomas Priermeier

Anorganisch-chemisches Institut der Technischen Universität München, Lichtenbergstrasse 4, D-85747 Garching, Germany

Received April 26, 1994®

Salt elimination between X–Al[$(CH_2)_3NMe_2$](R) and Y–Al(X)$_2$(Do) (X, Y = H, Cl, Br; R = Cl, Br, ^{i}Bu, $CH_2{}^t$Bu; Do = NMe_3, quinuclidine, THF) and [L(CO)$_n$M][K] (M = Fe, Ru, Co; L = CO, PMe_3, η^5-C_5H_5; n = 1–3) in THF solution quantitatively gives the transition-metal-substituted alanes L(CO)$_n$M–Al[$(CH_2)_3NMe_2$](R) (**2a–h**) and L(CO)$_n$M–Al(X)$_2$(Do) (**2k–m**). The new compounds were characterized by means of elemental analysis and ^{1}H, ^{13}C, ^{31}P, and ^{27}Al NMR, EI-MS, and infrared ν(CO) and ν(Al–H) data. **2a–m** constitute rare examples of nonbridged direct transition-metal–aluminum bonds. Those bonds are rather polarized in a $Fe^{\delta-}$–$Al^{\delta+}$ fashion and are thus highly reactive toward cleavage in the course of electrophilic or nucleophilic attack. X-ray single crystal data for **2a**, $(\eta^5\text{-}C_5H_5)(CO)_2$-Fe–Al[$(CH_2)_3NMe_2$](^{i}Bu): monoclinic, $P2_1/n$, a = 868.0(2) Å, b = 13.468(2) Å, c = 15.213(3) Å, β = 101.79(1)°, V = 1741 Å^3, Z = 4, R = 0.0536 (R_w = 0.0483). The σ(Fe–Al) bond length is 2.456(1) Å. **2a–d** are used as candidates to generate intermetallic Fe/Al and Co/Al thin films by low-pressure MOCVD.

Introduction

The development of organoaluminum chemistry has largely been driven by the use of these materials in catalysis. Currently, new but not less sophisticated utilizations have emerged, namely as volatile sources for aluminum-containing thin films for microelectronics.[1] These applications have especially renewed interest in the chemistry of alane and its derivatives.[2] For example, H_3AlNMe_3 has been shown to be an excellent molecular precursor for the deposition of highly pure aluminum by MOCVD (metal organic chemical vapor deposition) and other related techniques.[3] We were attracted to organoaluminum chemistry, since it was recently recognized that heteronuclear organometallics containing certain combinations of transition metals and group 13 metals may serve as so called "single-source precursors" to deposit the respective *mixed-metal* thin films.[4] Aluminides such as NiAl, CoAl, MnAl, etc., for example, are of interest for advanced metal-based transistor devices, e.g. as quantum wells for resonant tunneling diodes.[5] However, to be eligible for OMCVD, such organometallic compounds have to meet important requirements,[6] including (i) appropriate metal ratio, (ii) volatility, (iii) low heteroatom content in the ligand sphere ("all hydrocarbon precursors"[7]), (iv) facile pyrolysis (T < 400 °C) and controlled deposition chemistry to yield the pure intermetallic phase, (v) high purity, (vi) long-term stability, and last not least (vii) low-cost and high-yield synthesis. We have shown previously that transition-metal-substituted gallanes and indanes can be derived which fit into this scheme of properties.[8] Herein we wish to report our studies on stabilizing organoaluminum fragments at transition-metal centers also, aiming at sufficiently volatile and stable compounds with direct transition-metal to aluminum bonds which might be suitable for OMCVD of aluminum-containing thin alloy films.

Experimental Section

All manipulations were undertaken utilizing standard Schlenk, high-vacuum line, and glovebox techniques under an inert-gas atmosphere (purified argon). However, for the synthesis of **2a–m** a modified special reaction vessel[9] had to be employed to minimize undesired hydrolysis of the extremely air-sensitive compounds. The two arms (length 25 cm, i.d. 45 mm) of the vessel are attached to each other in a 120° angle

† IXth communication of the series organo group 13 transition metal Complexes. VIIIth communication see ref.[52]

® Abstract published in *Advance ACS Abstracts,* September 15, 1994.

(1) Stringfellow, G. B. *Organometallic Chemical Vapor Epitaxy*; Academic Press, New York, 1989.

(2) Atwood, J. L.; Bennett, F. R.; Jonas, C.; Koutsantonis, G. A.; Raston, C. L.; Robinson, K. D. *J. Chem. Soc., Chem. Commun.* **1992**, 541–543. Elms, F. M.; Lamb, R. N.; Pigram, P. J.; Gardiner, M. G.; Wood, B. J.; Raston, C. L. *J. Chem. Soc., Chem. Commun.* **1992**, 1423–1425. Atwood, J. L.; Bennett, F. R.; Elms, F. M.; Jones, C.; Raston, C. L.; Robinson, K. D. *J. Am. Chem. Soc.* **1991**, *113*, 8183–8185.

(3) Gladfelter, W. L.; Boyd, D. C.; Jensen, K. F. *Chem. Mater.* **1989**, *1*, 339–343. Baum, T. H.; Larson, C. E.; Jackson, R. L. *Appl. Phys. Lett.* **1989**, *55*, 1264–1266.

(4) Maury, F.; Brandt, L.; Kaesz, H. D. *J. Organomet. Chem.* **1993**, *449*, 159–165. Kaesz, H. D.; Williams, R. S.; Hicks, R. F.; Zink, J. I.; Chen, Y.-J.; Müller, H.-J.; Xue, Z.; Xu, D.; Shuh, D. K.; Kim, Y. K. *New J. Chem.* **1990**, *14*, 527–534.

(5) Harbinson, J. P.; Sands, T.; Ramesh, R.; Tabatabaie, N.; Gilchrist, H. L.; Florenz, L. T.; Keramidas, V. G. *J. Vac. Sci. Technol.* **1990**, *B8*, 242–245 and references cited therein. Williams, R. S. *Appl. Surf. Sci.* **1992**, *60/61*, 613–618 and references cited therein.

(6) Zanella, P.; Rossetto, G.; Brianese, N.; Ossola, F.; Porchia, M.; Williams, J. O. *Chem. Mater.* **1991**, *3*, 225–242. Maury, F. *Adv. Mater.* **1992**, *4*, 542–548.

(7) Zinn, A.; Niemer, B.; Kaesz, H. D. *Adv. Mater.* **1992**, *4*, 375–378.

(8) Fischer, R. A.; Behm, J.; Priermeier, T.; Scherer, W. *Angew. Chem.* **1993**, *105*, 776–778; *Angew. Chem., Int. Ed. Engl.* **1993**, *32*, 772–774. Fischer, R. A. In *Chemical Perspectives of Microelectronic Materials III*; Abernathy, C. R., Bates, C. W., Jr., D. A., Hobson, W. S., Eds.; Materials Research Society Symposium Proceedings 282; pp 267–273. Fischer, R. A.; Scherer, W.; Kleine, M. *Angew. Chem.* **1993**, *105*, 778–780; *Angew. Chem., Int. Ed. Engl.* **1993**, *32*, 774–776.

(9) Strohmeier, W. *Chem. Ber.* **1955**, *88*, 1218–1223.

0276-7333/94/2313-4306$04.50/0

Table 1. Numbering Pattern for the Compounds of Scheme 1[a]

compd	X	R	M	L	*n*	Do
1a	Br	^{i}Bu				
1b	Br	neo-Pe				
1c	Cl					
1d	Br					
1e	Cl					NMe_3
1f[b]	H					NC_7H_{13}
1g[b]	H					NMe_3
2a		^{i}Bu	Fe	Cp	2	
2b		neo-Pe	Fe	Cp	2	
2c		BH_4	Fe	Cp	2	
2d		^{i}Bu	Co	PMe_3	3	
2e		neo-Pe	Co	PMe_3	3	
2f	Br		Fe	Cp	2	
2g	Cl		Ru	Cp	2	
2h	Br		Co	PMe_3	3	
2k	Cl		Fe	Cp	2	THF
2l	H		Fe	Cp	2	NC_7H_{13}
2m	H		Fe	Cp	2	THF

[a] Abbreviations are as follows: Me, CH_3; ^{i}Bu, CH_2CHMe_2; neo-Pe, CH_2CMe_3; Cp, η^5-C_5H_5; NC_7H_{13}, quinuclidine. [b] Y = Br.

and separated by a D3 glass frit. The first part is equipped with two ground-glass joints, to which two side-arm dumpers are attached. A 50 mL round-bottom flask is mounted to the second part of the vessel in the same manner. The whole reaction vessel is flexibly (270°) connected to a greaseless high-vacuum line[10] (base pressure $<10^{-4}$ Torr). The glass surface of the reaction vessel was passivated by silylation with Me_2SiCl_2. Solvents were dried under argon by standard methods: *n*-pentane and toluene were stored over powdered molecular sieves (4 Å, Merck); diethyl ether and THF were stored over potassium benzophenone ketyl (residual water <1 ppm, Karl Fischer). Immediately prior to use, the solvents were condensed onto activated Al_2O_3 to remove the last traces of water and other impurities. Infrared spectra were recorded as thin films (Nujol mull) or solutions between carefully dried CaF_2 plates with a Nicolet FT-5DX instrument (sample preparation in the glovebox). JEOL JNM-GX400 and JNM-GX270 spectrometers were used for NMR spectroscopy. ^{1}H and ^{13}C NMR spectra were referenced to internal solvent and corrected to TMS. Other references used were as follows: ^{31}P NMR spectra, 80% aqueous H_3PO_4; ^{27}Al NMR spectra, aqueous solution of $[Al(H_2O)_6](NO_3)_3$, c = 1.0 M; ^{11}B NMR spectra, aqueous solution of H_3BO_4 (10%), set at −18.2 ppm. All samples for NMR spectra were contained in high-vacuum-sealed NMR tubes, using carefully dried deuterated solvents. Mass spectra were recorded using a Varian MAT 311-A instrument (EI spectra) and with a Varian MAT FS-90 instrument; *m/z* values are reported for ^{27}Al, ^{56}Fe, and ^{59}Co, with the normal isotope distribution being observed. Melting points were measured using sealed capillaries and are not corrected. Abbreviations are as follows: Me, CH_3; Et, C_2H_5; Ph, C_6H_5; ^{i}Bu, isobutyl; ^{t}Bu, *tert*-butyl; neo-Pe, neopentyl. Elemental analyses were provided by the Microanalytic Laboratory of the Technical University at Munich. The numbering scheme of the compounds is given in Table 1. The starting aluminum compounds **1c,d**[11] and **1e−g**[12] were synthesized according to literature procedures.

Synthesis of the Compounds 1a,b. A 1.53 g (6.36 mmol) sample of trineopentylaluminum[13] and a 3.40 g (12.75 mmol) sample of freshly sublimed $AlBr_3$ were each dissolved in 10 mL of *n*-pentane and were then slowly combined at −78 °C with vigorous stirring. The mixture was allowed to stand at room temperature overnight. After removal of the solvent the crude product was purified by short-path distillation at 85 °C (10^{-2} Torr dynamic vacuum). The product dibromoneopentylaluminum was obtained as a tan low-melting oil (4.60 g, 17.8 mmol, 93%) and was transferred into a round-bottom flask (250 mL). After dissolution in 50 mL of diethyl ether at −78 °C, solid [3-(dimethylamino)propyl]lithium[14] (1.64 g, 17.6 mmol) was slowly added with vigorous stirring. The mixture was then warmed to room temperature over 1 h, and the solvent was removed via vacuum distillation. The milky white oil was treated with 50 mL of toluene. The resulting white suspension was stirred for 5 h, after which time it was filtered and the solvent was removed. Short-path distillation at 91 °C (10^{-2} Torr) yielded the pure product **1b** as low-melting, large, colorless crystals (4.50 g, 95%). The compound **1a** was prepared analogously but was not characterized; it was used immediately after preparation.

1b: ^{1}H NMR (399.78 MHz, toluene-d_8, 25 °C; δ): 0.25, 0.55 [d, 14 Hz, 2H, $AlCH_2C(CH_3)_3$]; 0.28−0.36, 0.42−0.55 (AA′BB′, 2H, $AlCH_2CH_2$); 1.24 (AA′BB′CC′, br, 2H, $CH_2CH_2CH_2$); 1.27 [s, 9H, $C(CH_3)_3$]; 1.51−1.62, 2.20−2.28 (AA′BB′, 2H, CH_2CH_2N); 1.49, 1.95 (s, 6H, NCH_3). ^{13}C NMR (100.5 MHz, toluene-d_8, 25 °C; δ): 5.9 (t, br, $AlCH_2CH_2$); 21.1 (t, $CH_2CH_2CH_2$); 29.7 [t, br, $AlCH_2C(CH_3)_3$]; 31.2 (s, $CH_2C(CH_3)_3$); 34.9 [q, $C(CH_3)_3$]; 43.5, 46.8 (q, NCH_3); 62.9 (t, CH_2CH_2N). Anal. Calcd for $C_{10}H_{23}AlBrN$ (M_r = 264.18): C, 45.46; H, 8.78; N, 5.30; Br, 30.25; Al, 10.21. Found: C, 45.27; H, 8.65; N, 5.19; Br, 30.33; Al, 9.50.

Synthesis of Compounds 2a−m. The compounds **2a−m** were all synthesized according to the procedure for the synthesis of **2f** outlined below. Using the reaction vessel described above, 50 mL of THF was condensed onto potassium graphite (C_8K; 0.79 g, 5.6 mmol). The golden brownish suspension was cooled to −78 °C, and a 0.92 g (2.6 mmol) sample of solid $[(\eta^5\text{-}C_5H_5)(CO)_2Fe]_2$ was added via a side-arm dumper. The mixture was then vigorously stirred and warmed to room temperature within 30 min. The obtained solution of $[(\eta^5\text{-}C_5H_5)(CO)_2Fe]K$ ($c \approx 0.1$ M) was cooled again to −78 °C, and a 1.41 g (5.2 mmol) sample of $Br_2Al[(CH_2)_3NMe_2]$[11] (dissolved in ca. 10 mL of THF) was quickly added in one portion via the second side-arm dumper. The color of the reaction mixture changed immediately from deep brown to black (suspended graphite). The stirred mixture was warmed to room temperature within 30 min. The solvent was then removed, and the residue was dried in vacuo. A mixture of 40 mL of *n*-pentane/toluene (2:1) was then condensed onto the black residue. The extract was filtered through the glass frit into the second arm of the reaction vessel. The solvent mixture was then condensed back into the first side arm of the reaction vessel, and the extraction of the product was repeated as before. After three extraction cycles the solvent was removed in vacuo. The product was washed at −10 °C with 5 mL of *n*-pentane (condensed onto the reddish brown crude product) to remove traces of $[(\eta^5\text{-}C_5H_5)(CO)_2(Fe)_2$, $(\eta^5\text{-}C_5H_5)(CO)_2Fe{-}H$, $Br_2Al[(CH_2)_3NMe_2]$, and "$Br(HO)Al[(CH_2)_3NMe_2]$". The washing solution was decanted off and filtered back into the first arm of the reaction vessel. The washing cycle was repeated five times. The purified off-white microcrystalline product was dissolved in 10 mL of toluene and transferred into a 50 mL round-bottom flask which was attached to the second side arm of the reaction vessel. The product was crystallized at 25 °C by slow evaporation of the solvent over 2 days. The nearly colorless crystals obtained were washed with 5 mL of *n*-pentane (−10 °C) and dried in vacuo. Yield: 1.57 g (82%). **2g,k−m** were obtained analogously. The compounds **2a,b** were synthesized either by following the above procedure using **1a** or **1b** as the starting organoaluminum compound or by treating **2f** with an equimolar amount of solid LiR in diethyl ether at 25 °C for 5 h. **2f** itself was also prepared by treating

(10) Wada, A. L.; Dye, J. L. *J. Chem. Educ.* **1985**, *62*, 356−358.
(11) Schumann, H.; Hartmann, U.; Wassermann, W.; Just, O.; Dietrich, A.; Pohl, L.; Hostalek, M.; Lokai, M. *Chem. Ber.* **1991**, *124*, 1113−1119.
(12) Ruff, J. K. *J. Am. Chem. Soc.* **1961**, *83*, 1798−1800. Ruff, J. K.; Hawthorne, M. F. *J. Am. Chem. Soc.* **1960**, *82*, 2141−2144. Atwood, J. L.; Butz, K. W.; Gardiner, M. G.; Jones, C.; Koutsantonis, G. A.; Raston, C. L.; Robinson, K. D. *Inorg. Chem.* **1993**, *32*, 3482−3487 and references cited therein.
(13) Beachley, O. T.; Victoriano, L. *Organometallics* **1988**, *7*, 63−67.
(14) Thiele, K.-H.; Langguth, E.; Müller, G. E. *Z. Anorg. Allg. Chem.* **1980**, *462*, 152−156.

2k with an equimolar amount of solid Li[$(CH_2)_3NMe_2$] in diethyl ether at 25 °C for 5 h. The good solubility of **2a,b** in saturated hydrocarbons required that these compounds had to be crystallized from saturated *n*-heptane solutions by slow cooling to −78 °C over several weeks (typical yield: 50−70%, as nearly colorless crystals). We have not been able to obtain satisfactory elemental analyses for **2a,b,m** so far ($\Delta C \geq 0.7\%$), which is probably due to the extreme air and moisture sensitivity of these compounds, which apparently caused some decomposition during sample preparation for microanalysis. Compound **2c** could not be obtained in pure form by treatment of **2f** with a large excess of Li[BH_4] in diethyl ether over 24 h at 25 °C and was always contaminated with **2f**. By the procedure for **2f** the CoAl compounds **2d,e,h** were synthesized using [$Me_3P(CO)_3Co$]K.[15] The potassium graphite reduction to synthesize the transition-metal nucleophile in situ was not necessary in these cases, of course. Selected analytical and spectroscopic data for **2a−m** are as follows.

2a: pale yellow crystals. ^{13}C NMR (100.5 MHz, C_6D_6, 25 °C; δ): 9.6 (t, br, $AlCH_2CH_2$); 22.6 (t, $AlCH_2CH_2$); 27.4 (d, $AlCH_2CH$); 28.6 [q, $CH(CH_3)_2$]; 29.0 (t, br, $AlCH_2C$); 46.7, 46.9 (q, NCH_3); 64.9 (t, NCH_2); 81.2 (d, C_5H_5); 219.4, 291.0 (s, FeCO). $^{27}Al\{^1H\}$ NMR (104.14 MHz, C_6D_6, 25 °C; δ): 210 ($F_{1/2}$ = 3600 Hz). IR (*n*-pentane): ν(CO) 1964 vs, 1953 vs, 1905 vs, 1892 vs cm^{-1}.

2b: pale yellow crystals. ^1H NMR (399.78 MHz, C_6D_6, 25 °C; δ): 0.46, 0.76 (s, 2 H, $AlCH_2CMe_3$); 0.51, 0.63 (AA′BB′, 2 H, $AlCH_2$); 1.20 [s, 9 H, $C(CH_3)_3$]; 1.60, 1.78 (AA′BB′CC′, 2 H, $AlCH_2CH_2$); 2.02, 2.59 (AA′BB′, 2 H, CH_2N); 1.90, 2.03 (s, 6 H, NCH_3); 4.27 (s, 5 H, C_5H_5). ^{13}C NMR (100.5 MHz, C_6D_6, 25 °C; δ): 11.2 (t, br, $AlCH_2CH_2$); 22.6 (t, $AlCH_2CH_2$); 31.9 (s, $AlCH_2C$); 34.9 [q, $(C(CH_3)_3]$; 35.3 (t, br, $AlCH_2C$); 47.5, 47.7 (q, NCH_3); 65.0 (t, NCH_2); 81.5 (d, C_5H_5); 219.5, 219.2 (s, FeCO). $^{27}Al\{^1H\}$ NMR (104.14 MHz, C_6D_6, 25 °C; δ): 214 ($F_{1/2}$ = 3470 Hz). IR (*n*-pentane): ν(CO) 1965 vs, 1954 vs, 1906 vs, 1893 vs cm^{-1}.

2c: ^1H NMR (399.78 MHz, C_6D_6, 25 °C; δ): 0.50, 0.65 (AA′BB′, 2 H, $AlCH_2$); 1.42, 1.60 (AA′BB′CC′, 2 H, $AlCH_2CH_2$); 2.07, 2.18 (AA′BB′, 2 H, CH_2N); 1.91, 1.93 (s, 6 H, NCH_3); 4.31 (s, 5 H, C_5H_5). ^{13}C NMR (100.5 MHz, C_6D_6, 25 °C; δ): 10.8 (t, br, $AlCH_2$); 21.2 (t, $AlCH_2CH_2$); 45.6, 47.0 (q, NCH_3); 63.7 (t, NCH_2); 81.9 (d, C_5H_5); 217.9, 217.4 (s, FeCO). $^{27}Al\{^1H\}$ NMR (104.14 MHz, C_6D_6, 25 °C; δ): 207 ($F_{1/2}$ = 1950 Hz). ^{11}B NMR (128.3 MHz, C_6D_6, 25 °C; δ): −33.8 [quint, $^1J(B,H)$ = 84 Hz]. IR (Nujol): ν($B-H_t$) 2453 m, 2407 m cm^{-1}; ν(CO) 1964 br, vs, 1906 br, vs cm^{-1}.

2d: colorless crystals (*n*-pentane); mp 35 °C; sublimes at 60 °C, 10^{-3} Torr. ^1H NMR (399.78 MHz, C_6D_6, 25 °C; δ): 0.45, 0.74 [dd, 2H, $^1J(H,H)$ = 13.7 Hz, $^3J(H,H)$ = 6.5 Hz, $AlCH_2$]; 0.86 [m, 1H, $^3J(H,H)$ = 6.5 Hz, CH_2CHMe_2]; 0.82−0.93 (AA′BB′, 2H, $AlCH_2CH_2$); 1.07 [d, 9H, $^2J(P,H)$ = 8.6 Hz, $P(CH_3)_3$]; 1.32 [t, 6H, $^3J(H,H)$ = 6.5 Hz, $CH(CH_3)_2$]; 1.61−1.72, 1.76−1.84 (AA′BB′CC′DD′, 2H, $AlCH_2CH_2$); 1.99, 2.23 (s, 6H, NCH_3); 2.01−2.10, 2.25−2.31 (AA′BB′, 2H, CH_2N). ^{13}C NMR (100.5 MHz, C_6D_6, 25 °C; δ): 9.8 (br, $AlCH_2CH_2$); 20.2 [dq, $^1J(P,H)$ = 26.7 Hz, $P(CH_3)_3$]; 22.5 (t, $AlCH_2CH_2$); 28.3 (d, CH_2CHMe_2); 28.9 [q, $CH(CH_3)_2$]; 46.7, 46.8 (q, NCH_3); 64.9 (t, NCH_2); 205.6 [d, $^2J(P,C)$ = 41 Hz, CoCO]. $^{27}Al\{^1H\}$ NMR (104.14 MHz, C_6D_6, 25 °C; δ): 199 ($F_{1/2}$ = 4360 Hz). $^{31}P\{^1H\}$ NMR (161.9 MHz, C_6D_6, 25 °C; δ): 9.0. IR (*n*-pentane): ν(CO) 1923 sst, 1904 sst cm^{-1}. Anal. Calcd for $C_{15}H_{30}AlCoNPO_3$ (M_r = 389.29): C, 46.15; H, 7.54; N, 3.39; Co, 14.80. Found: C, 46.28; H, 7.77; N, 3.60; Co, 15.14.

2e: colorless crystals (*n*-pentane); mp 35 °C; sublimes at 60 °C, 10^{-3} Torr. ^1H NMR (399.78 MHz, C_6D_6, 25 °C; δ): 0.66, 0.95 (d, 2H, 14.1 Hz, $AlCH_2$); 0.72, 0.84 (AA′BB′, 2H, $AlCH_2CH_2$); 1.09 [d, 9H, $^2J(P,H)$ = 8.5 Hz, $P(CH_3)_3$]; 1.29 [s, 9H, $C(CH_3)_3$]; 1.66, 1.81 (m, 1 H, $AlCH_2CH_2$); 2.06 (s, 3 H, NCH_3); 2.08 (m, 1 H, NCH_2CH_2); 2.27 (s, 3 H, NCH_3); 2.37 (m, 1 H, NCH_2CH_2). ^{13}C NMR (100.5 MHz, C_6D_6, 25 °C; δ): 11.4 (t, br, $AlCH_2CH_2$); 22.5 (t, $AlCH_2CH_2$); 32.2 [s, $AlCH_2C(CH_3)_3$]; 34.8 (q, CCH_3); 34.9 (t, br, $AlCH_2C$); 47.5, 47.7 (q, NCH_3); 65.0 (t, NCH_2); 205.8 [d, $^1J(P,C)$ = 8 Hz, CoCO]. $^{27}Al\{^1H\}$ NMR (104.14 MHz, toluene-d_8, 25 °C; δ): 198 ($F_{1/2}$ = 4340 Hz). $^{31}P\{^1H\}$ NMR (161.9 MHz, toluene-d_8, −80 °C; δ): 9.0. IR (*n*-pentane): ν(CO) 1922 sst, 1903 vs cm^{-1}. MS (EI, 70 eV, 90 °C; *m/z* (%)): 403 (2) [M^+]; 375 (1) [M^+ − CO]; 347 (2) [M^+ − 2 CO]; 332 (3) [$M^+ - CH_2C(CH_3)_3$]; 313 (49) [$(MH^+ - P(CH_3)_3 - CH_3$]; 76 (26) [$P(CH_3)_3^+$]; 57 (71) [$C(CH_3)_3^+$]; 58 (100) [$H_2CN(CH_3)_2^+$]. Anal. Calcd for $C_{16}H_{32}AlCoNPO_3$ (M_r = 403.32): C, 47.63; H, 8.00; N, 3.47; Co, 14.62. Found: C, 47.15; H, 7.54; N, 3.29; Co, 13.70.

2f: pale yellow to colorless crystals (tolene); mp 72 °C. ^1H NMR (399.78 MHz, C_6D_6, 25 °C; δ): 0.60, 0.76 (AA′BB′, 2H, $AlCH_2$); 1.47, 1.66 (AA′BB′CC′, 2H, $AlCH_2CH_2$); 1.78, 2.59 (AA′BB′, 2H, CH_2N); 1.94, 2.29 (s, 6H, NCH_3); 4.34 (s, 5H, C_5H_5). ^{13}C NMR (100.5 MHz, C_6D_6, 25 °C; δ): 10.8 (t, br, $AlCH_2$); 21.3 (t, $AlCH_2CH_2$); 44.3, 48.0 (q, NCH_3); 63.4 (t, NCH_2); 82.5 (d, C_5H_5); 217.7, 217.5 (s, FeCO). $^{27}Al\{^1H\}$ NMR (104.14 MHz, C_6D_6, 25 °C; δ): 197 ($F_{1/2}$ = 1880 Hz). IR [*n*-pentane (THF)]: ν(CO) 1968 (1965) vs, 1911 (1906) vs cm^{-1}. MS (EI, 70 eV, 60 °C; *m/z* (%)): 369 (0.5) [M^+]; 192 (5) [$BrAl[(CH_2)_3NMe_2^+]$; 121 (42) [$C_5H_5Fe^+$]; 58 (100) [$H_2CN(CH_3)_2^+$]. Anal. Calcd for $C_{12}H_{17}AlBrFeNO_2$ (M_r = 370.00): C, 38.95; H, 4.63; N, 3.79; Al, 7.29; Br, 21.60; Fe, 15.09. Found: C, 38.97; H, 4.78; N, 3.82; Al, 6.80; Br, 21.64; Fe, 15.44.

2g: nearly colorless crystals (toluene); mp 85 °C. ^1H NMR (399.78 MHz, C_6D_6, 25 °C; δ): 0.45, 0.66 (AA′BB′, 2H, $AlCH_2$); 1.35, 1.53 (AA′BB′CC′, 2H, $AlCH_2CH_2$); 1.72, 2.45 (AA′BB′, 2H, CH_2N); 1.96, 2.25 (s, 6H, NCH_3); 4.65 (s, 5H, C_5H_5). ^{13}C NMR (100.5 MHz, C_6D_6, 25 °C; δ): 10.5 (t, br, $AlCH_2$); 21.1 (t, $AlCH_2CH_2$); 44.4, 48.2 (q, NCH_3); 63.6 (t, NCH_2); 86.4 (d, C_5H_5); 212.6, 212.1 (s, RuCO). $^{27}Al\{^1H\}$ NMR (104.14 MHz, C_6D_6, 25 °C; δ): 192 ($F_{1/2}$ = 1820 Hz). IR (toluene): ν(CO) 1976 vs, 1915 vs cm^{-1}. Anal. Calcd for $C_{12}H_{17}AlClNO_2Ru$ (M_r = 370.78): C, 38.87; H, 4.62; Al, 7.28; Cl, 9.56; N, 3.78; Ru, 27.26. Found: C, 38.59; H, 4.57; Al, 7.36; Cl, 9.44; N, 3.69; Ru, 26.76.

2h: off-white microcrystalline powder (toluene/*n*-pentane); mp 75 °C; sublimes at 160 °C, 10^{-3} Torr. ^1H NMR (399.78 MHz, C_6D_6, 25 °C; δ): 0.93 (AA′BB′, 2H, $AlCH_2CH_2$); 0.97 [d, 9 H, $^2J(P,H)$ = 9.2 Hz, $P(CH_3)_3$]; 1.52, 1.65 (AA′BB′CC′, 2H, $AlCH_2CH_2$); 1.81, 2.53 (AA′BB′, 2H, NCH_2CH_2); 2.09, 2.40 (s, 6H, NCH_3). ^{13}C NMR (100.5 MHz, C_6D_6, 25 °C; δ): 11.0 (t, br, $AlCH_2CH_2$); 19.9 [qd, $^1J(P,C)$ = 28 Hz, $P(CH_3)_3$]; 21.2 (t, $AlCH_2CH_2$); 44.5, 48.2 (q, NCH_3); 63.4 (t, NCH_2); 205.8 [d, $^1J(P,C)$ = 8 Hz, CoCO]. $^{27}Al\{^1H\}$ NMR (104.14 MHz, C_6D_6, 25 °C; δ): 181 ($F_{1/2}$ = 1890 Hz). $^{31}P\{^1H\}$ NMR (161.9 MHz, C_6D_6, 25 °C; δ): 9.0. IR (*n*-pentane): ν(CO) 1928 sst, 1907 vs. Anal. Calcd for $C_{11}H_{21}AlBrCoNPO_3$ (M_r = 412.09): C, 32.06; H, 5.14; N, 3.40; Co, 14.30; Br, 19.39; Al, 6.55. Found: C, 31.85; H, 4.97; N, 3.25; Co, 13.90; Br, 19.21; Al, 6.30.

2k: off-white microcrystalline powder (toluene); mp 92 °C dec. ^1H NMR (399.78 MHz, C_6D_6, 25 °C; δ): 1.02 (t, 4H, OCH_2CH_2); 3.99 (t, 4H, OCH_2CH_2); 4.40 (s, 5H, C_5H_5). $^{27}Al\{^1H\}$ NMR (104.14 MHz, C_6D_6, 25 °C; δ): 185 ($F_{1/2}$ = 1590 Hz). ^{13}C NMR (100.5 MHz, C_6D_6, 25 °C; δ): 24.7 (t, OCH_2CH_2); 73.7 (t, OCH_2CH_2); 82.5 (d, C_5H_5); 216.4 (s, FeCO). $^{27}Al\{^1H\}$ NMR (104.14 MHz, C_6D_6, 25 °C; δ): 156 ($F_{1/2}$ = 1135 Hz). IR (toluene): ν(CO) 1981 sh, 1972 vs, 1923 sh, 1913 vs cm^{-1}. Anal. Calcd for $C_{11}H_{13}AlCl_2FeO_3$ (M_r = 346.96): C, 38.08; H, 3.78; Al, 7.78; Cl, 20.44; Fe, 16.10. Found: C, 37.93; H, 3.96; Al, 7.50; Cl, 21.15; Fe, 15.97.

2l: yellow microcrystalline powder (toluene); mp 80 °C dec. ^1H NMR (399.78 MHz, toluene-d_8, −85 °C; δ): 1.00 [m, br, 6H, $HC(CH_2)_3$]; 1.17 [m, br, 1H, $HC(CH_2)_3$]; 2.87 [m, br, 6H, $N(CH_2)_3$]; 4.29 (s, 5H, C_5H_5). ^{13}C NMR (100.5 MHz, C_6D_6, 25 °C; δ): 20.0 [d, $HC(CH_2)_3$], 24.9 [t, $HC(CH_2)_3$]; 47.9 (t, $N(CH_2)_3$]; 82.5 (d, C_5H_5); 219.3 (s, FeCO). $^{27}Al\{^1H\}$ NMR (104.14 MHz, C_6D_6, 25 °C; δ): 221 ($F_{1/2}$ = 2520 Hz). IR (toluene): ν(CO) 1953 br, vs, 1891 br, vs cm^{-1}; ν($Al-H_t$) 1748 cm^{-1}; ν($Al-D_t$) 1264 cm^{-1}. Anal. Calcd for $C_{14}H_{20}AlFeNO_2$ (M_r = 317.15): C, 53.02; H, 6.36; N, 4.42. Found: C, 52.74; H, 5.90; N, 3.80.

2m: yellow microcrystalline powder (toluene); dec >42 °C. ^1H NMR (399.78 MHz, C_6D_6, 25 °C; δ): 1.35 (s, br, 4H,

(15) Hammer, R.; Klein, H.-F. *Z. Naturforsch.* **1977**, *32B*, 138−143.

OCH_2CH_2); 2.09 [s, br, 4H, OCH_2CH_2); 3.88 (s, br, 2H, AlH); 4.47 (s, 5H, C_5H_5). IR (toluene): ν(CO) 1950 br, vs, 1890 br, vs cm^{-1}; ν(Al—H_t) 1752 cm^{-1}; ν(Al—D_t) 1268 cm^{-1}.

Single-Crystal Structure Analysis of 2a. Compound **2a** crystallizes from *n*-pentane as colorless prisms. A specimen of dimensions 0.230 × 0.102 × 0.205 mm was selected and transferred with cooling into a Lindemann capillary, which was subsequently sealed under argon and mounted onto a automatic four-circle diffractometer (CAD4 Enraf-Nonius; graphite-monochromated Mo Kα X-ray radiation: $\lambda = 7.1073$ Å). The extinctions ($h0l$, $h + l = 2n + 1$; $0k0$, $k = 2n + 1$) are consistent with the monoclinic space group $P2_1/n$ (No. 14[16]). The lattice constants were refined on the basis of 25 reflections ($30.09 < 2\theta < 41.7°$) to $a = 8.680(2)$ Å, $b = 13.468(2)$ Å, $c = 15.213(3)$ Å, $\beta = 101.79(1)°$, $V = 1741$ Å^3, $Z = 4$, and ϱ(calc) = 1.325 g cm^{-3} ($C_{16}H_{26}AlFeNO_2$, 347.22 amu). The cell parameters were checked with the cell reduction programs "TRACER"[17] and "LEPAGE".[18] The collection of the intensities was performed at 193 K within $1.0° \le \theta \le 25.0°$: h (0−10), k (0−16), l (−18 to +18); ω-scan mode, variable scan width [(0.6 + 0.35 tan θ)° ±25% before and after each reflection for background control], and a maximum time of measurement of $t_{max} = 60$ s. The intensity of the reflections and the orientation of the crystal during the measurement were routinely checked. Within 69 h each of three control reflections lost 5.8% of its initial intensity due to some degradation of the crystal. The decomposition was corrected anisotropically (program "CHORT"[17]). A total of 3417 intensities were measured, from which 526 with $I < 0$ were regarded as not observed. After Lp correction, empirical absorption correction ($\mu = 9.18$ cm^{-1} on the basis of ψ-scan data with the program "EAC";[17] transmission minimum/maximum 83.09%/99.84%) and averaging 2558 independent reflections remained, of which 2350 (NO) with $I > 0.5\sigma(I)$ were used for the structure solution and refinement. A total of 253 (NV) parameters were refined by full-matrix least squares. The structure solution was performed with Patterson methods[19] and subsequent difference Fourier techniques.[20] In the asymmetric unit 17 positions of heavy atoms were refined by full-matrix least squares with anisotropic thermal parameters, and 8 positions of carbon atoms C41 to C72 were refined isotropically with occupation factors less than 1.0. Atom form factors for neutral atoms[21] and anomalous dispersion were considered.[22] Sixteen hydrogen atom positions were obtained from difference Fourier syntheses and were refined freely. A total of 20 hydrogen atom positions located at disordered carbon atoms were placed in ideal geometry with collective isotropic thermal parameters (and the respective occupational parameters) and included in the structure factor calculations, but not refined. The weighting scheme described by Tukey and Prince[23] with three refined parameters ($p(1) = 0.671$, $p(2) = 0.258$, $p(3) = 0.355$) was applied. The Larson extinction parameter[24] was 14.766. In the last cycle of the structure refinement (program system "Platon"[18]) the shift/error was less than 0.0001 and a residual electron density of +0.44 e Å^{-3} remained, located 109 Å beneath the heavy atom Fe. $R = \Sigma(||F_o| - |F_c||)/\Sigma|F_o| = 0.0536$; $R_w = [\Sigma w(|F_o| - |F_c|)^2/\Sigma w|F_o|^2]^{1/2} = 0.0483$; GOF = $[\Sigma w(|F_o| - |F_c|)^2(NO - NV)]^{1/2} = 3.772$. The five-membered heterocyclic chelate ring of **2a** is disordered. The disorder was resolved for the atoms C41/C42, C51/C52, C61/C62, and C71/C72. In Table 2 the fractional atomic coordinates for compound **2a** are given. For C3 and N1 the disorder could not be fully resolved, which caused significant geometric distortions of the C—C and C—N bond geometries in the case of freely refined atomic positions. The structural features of this part of the molecule **2a**, however, are very similar to the known structures of closely related systems. For this reason restrictions to fix the geometry were not applied for the structure solution of **2a**. The principal geometric parameters of **2a**, e.g. the entries of Table 3, proved to not be significantly affected by the disorder of the chelate ring.

Table 2. Fractional Atomic Coordinates and Equivalent Isotropic Thermal Parameters for the Non-Hydrogen Atoms of 2a

atom	*x/a*	*y/b*	*z/c*	*U*(eq)[a] (Å^2)
Fe1	0.24316(6)	0.06263(4)	0.12076(3)	0.0299
C1	0.3740(5)	−0.0204(3)	0.0883(3)	0.0379
C2	0.1617(5)	−0.0286(3)	0.1781(2)	0.0348
C3	0.5537(5)	−0.0679(3)	0.2964(3)	0.0418
C8	0.3705(5)	0.1355(3)	0.3607(3)	0.0347
C9	0.2204(5)	0.1000(3)	0.3900(3)	0.0381
C10	0.2399(7)	−0.0035(4)	0.4300(3)	0.0486
C11	0.1698(8)	0.1711(5)	0.4570(4)	0.0582
C15	0.2567(6)	0.2179(3)	0.1284(3)	0.0424
C16	0.1075(6)	0.1866(3)	0.1385(3)	0.0457
C17	0.0351(6)	0.1359(4)	0.0589(3)	0.0502
C18	0.1403(6)	0.1357(3)	0.0005(3)	0.048
C19	0.2774(6)	0.1855(3)	0.0433(3)	0.0424
C41	0.709(1)	−0.057(1)	0.281(1)	0.0535*
C51	0.766(1)	0.0498(8)	0.3118(8)	0.0514*
C61	0.682(1)	0.2183(8)	0.3079(7)	0.0351*
C71	0.684(1)	0.134(1)	0.1690(7)	0.0481*
Al1	0.4377(1)	0.05894(8)	0.26281(7)	0.0272
O1	0.4592(4)	−0.0770(2)	0.0657(2)	0.0578
O2	0.1021(4)	−0.0897(2)	0.2137(2)	0.0505
N1	0.6519(4)	0.1237(2)	0.2510(2)	0.0394

[a] Values for anisotropically refined atoms are given in the form of the isoropic equivalent thermal parameter, defined as one-third of the trace of the orthogonalized U. Starred values denote atoms refined isotropically.

Table 3. Selected Interatomic Distances (Å) and Angles (deg) for 2a

Bond Distances					
Fe1—Al1	2.456(1)	Al1—C3	1.997(4)	Fe1—Cp	1.723(-)
Fe1—C1	1.736(4)	Al1—C8	1.993(4)	C1—O1	1.162(5)
Fe1—C2	1.739(4)	Al1—N1	2.094(3)	C2—O2	1.162(5)
Bond Angles					
C2—Fe1—C1	92.5(2)		N1—Al1—Fe1		112.3(1)
Al—Fe1—C1	82.2(1)		N1—Al1—C3		88.2(2)
Al—Fe1—C2	79.7(1)		N1—Al1—C8		104.4(2)
Cp—Fe1—Al1	121.8(-)		C3—Al1—Fe1		117.6(2)
Cp—Fe1—C1	131.7(-)		C8—Al1—Fe1		113.2(1)
Cp—Fe1—C2	130.0(-)		C8—Al1—C3		117.4(2)
Torsion Angles					
C1—Fe1—Al1—N1	67.6(-)		C2—Fe1—Al1—N1		161.6(-)
C1—Fe1—Al1—C8	−174.5(-)		C2—Fe1—Al1—C8		−80.5(-)
C1—Fe1—Al1—C3	−32.4(-)		C2—Fe1—Al1—C3		61.6(-)

MOCVD Experiments. CVD experiments were carried out in a nearly isothermal horizontal hot wall quartz tube reactor (length 30 cm; i.d. 3 cm; base pressure $<10^{-5}$ Torr) which was charged with various cleaned substrates (borosilicate glass, quartz slides, stainless steel, Si(100), GaAs(100), and KBr pellets). At typically 2.5 × 10^{-3} Torr dynamic vacuum, the source compound sublimed from a thermostated reservoir (25−80 °C) into the preheated deposition zone (length 15 cm), which was kept at constant temperature between 200 and 500 (±10) °C. No carrier gas was used. Volatile byproducts, which collected in a cold trap (−196 °C) connecting the reactor and the vacuum pump, were isolated, separated, and characterized by spectroscopic (NMR, MS) and analytical

(16) *International Tables of X-Ray Crystallography*; Kynoch Press: Birmingham, England, 1974; Vol. I.
(17) Frenz, B. A. The Enraf-Nonius CAD4 SDP System. In *Computing in Crystallography*; Delft University Press: Delft, Holland, 1978.
(18) Spek, A. L. The "EUCLID" Package. In *Computational Crystallography*; Sayre, D., Ed.; Clarendon Press: Oxford, England, 1982; p 528.
(19) Sheldrick, G. M. SHELXS-86, Program for Crystal Structure Determination; Universität Göttingen: Göttingen, Germany, 1986.
(20) Watkin, D. J.; Betteridge, P. W.; Carruthers, J. R. *CRYSTALS User Manual*; Oxford University Computing Laboratory: Oxford, England, 1986.
(21) Cromer, D. T.; Waber, J. T. *International Tables of X-Ray Crystallography*; Kynoch Press: Birmingham, England, 1974; Vol. IV, Table 2.2.B.
(22) Cromer, D. T. *International Tables of X-Ray Crystallography*; Kynoch Press: Birmingham, England, 1974; Vol. IV, Table 2.3.1.
(23) Prince, E. *Mathematical Techniques in Crystallography*; Springer-Verlag; Berlin, 1982.
(24) Larson, A. C. *Crystallographic Computing*; Munksgaard: Copenhagen, Denmark, 1969.

Scheme 1. Synthesis of the Compounds 2a–m

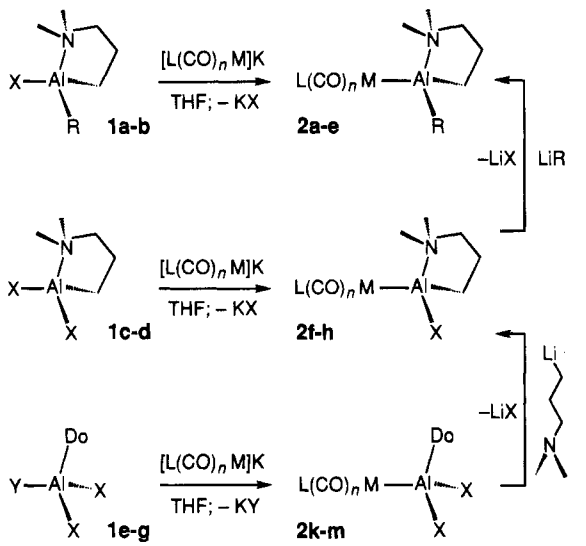

techniques (GC/MS). The films obtained were examined by AAS (after dissolution of the film with HNO_3), SEM-EDX, AES, and XRD. The thin-film compositions did not vary significantly over the coated areas (3.5 cm^2; AES, SEM-EDX).

Results and Discussion

A. Synthesis and Properties. When equimolar quantities of the (intramolecular) base-stabilized aluminum halides **1a–g** were combined with transition-metal carbonylates $[L(CO)_nM][K]$ (M = Fe, Ru, Co; L = CO, PMe_3, η^5-C_5H_5; n = 1–3) in THF solution, one halide group at the aluminum center was selectively and almost instantaneously substituted by the transition-metal fragment even at dry ice temperature (Scheme 1, Table 1) to yield the new compounds **2a–m**. No side products, e.g. multiple substitution or attack at the carbonyl substituents, were detected by IR spectroscopy of the reaction solutions, except for traces of $L(CO)_nM$–H, which arose from hydrolysis during the transfer of the solution into the IR cell. The remaining halide functionalities of **2f–h** were exchanged in subsequent steps by various residues. A quantitative introduction of the $[BH_4^-]$ substituent to yield **2c** failed, however. Even with a 10-fold excess of $Li[BH_4]$ in diethyl ether the molar ratio **2c**:**2f** was still not better than 1:1. (An exchange of Br^- against Cl^- for **2f** gave no better yields of **2c**.) This result differs from the related Fe–Ga chemistry. In that case the gallium analogue of **2c**, (η^5-C_5H_5)$(CO)_2$Fe–Ga[$(CH_2)_3NMe_2$](η^2-BH_4), was obtained quantitatively,[25] with just 1 equiv of $Li[BH_4]$. With rigorous exclusion of air and moisture analytically pure, nearly colorless crystalline samples of **2a–m** (except **2c**) were obtained in good yields of typically 80–90%. The compounds sublimed unchanged under moderate conditions (10^{-3} Torr, 60–100 °C; except **2l**,**m**) and were soluble in all common aprotic organic solvents. The intermetallic bonds in these new M–Al complexes were rapidly cleaved by Me_3SnCl to quantitatively yield $L(CO)_nM$–$SnMe_3$, Cl–Al[$(CH_2)_3NMe_2$](R), and Cl–Al$(X)_2$(Do), respectively.

Similar salt elimination reactions have been widely used in transition-metal boron, gallium, indium, and thallium chemistry to obtain metal–metal-bonded systems.[26] Interestingly, the synthesis of the few previously known transition-metal–aluminum bonds followed other distinct routes, which were typically based on Al–C bond cleavage or Lewis acid/base adduct formation at the transition-metal center. Structurally characterized examples include some transition-metal aluminum clusters, e.g. $C_{25}H_{35}Al_3MO_2$ (M = Mo, W),[27] $C_{26}H_{34}Al_4Mo$,[28] and $C_{28}H_{40}Al_2Ti_2$,[29] the dinuclear compounds (PNP)Ir($AlMe_2$)CMe=CH_2 (PNP = N[$SiMe_2CH_2PPh_2]_2$,[30] hydrogen-bridged complexes, e.g. ($H_{13}C_7N$)-(Me_2)Al(μ-H)Ni(η^6-*trans,trans,trans*-1,5,9-cyclododecatriene),[31] and species such as [(η^5-C_5Me_5)(Me_3)M]$_2AlMe_2$ (M = Rh, Ir)[32] and (η^5-C_5H_5)$(PMe_3)_2$Rh–$Al_2Me_4Cl_2$).[33] A typical property of such complexes is the *absence* of carbonyl groups. Otherwise, the isocarbonyl structure E–OC–M is the predominant bonding type. Lewis acidic oxophilic metal centers (E) usually attack the hard oxygen atoms in Lewis basic carbonyl complexes rather than the softer metal centers (M).[34] Consequently, the combination of the weak transition-metal nucleophiles $[L(CO)_nM]K$ (n = 3, L = η^5-C_5H_5, M = Cr, Mo, W; n = 4, 5, L = CO, M = Co, Mn), exhibiting high charge density at the carbonyl substituents,[35] with the aluminum halides **1a–f** did not give the metal–metal-bonded systems. The preference of the M–Al coordination over the usual M–CO–Al isocarbonyl structure can be achieved by adjustment of the Lewis acid/base properties at both metal centers: use of strong transition-metal nucleophiles, e.g. [(Me_3P)$(CO)_3$Co][K] rather than [$(CO)_4$Co][K], and preferably nitrogen donor stabilization at the aluminum center. By similar concepts the first structurally characterized example of an *non-bridged* lanthanide–transition-metal bond, (η^5-C_5H_5)-$(CO)_2$Ru–Lu(η^5-C_5H_5)$_2$(THF), has recently been obtained,[34] which constitutes a direct lanthanide analogue of **2a–m**. The presence of chelating alkyl substituents at the aluminum is not a necessary requirement, as the entries in Scheme 1 show; however, it adds some stability against the influence of air and moisture. Particularly noteworthy is the compound **2k**, (η^5-C_5H_5)$(CO)_2$Fe–$AlCl_2$(THF), which is the first aluminum congener of the already known gallium systems $L(CO)_nM$–$GaCl_2$(Do).[36] **2k** was synthesized in situ and

(25) Fischer, R. A.; Priermeier, T.; Scherer, W. *J. Organomet. Chem.* **1993**, *459*, 65–71.

(26) Taylor, M. J. *Metal to Metal Bonded States of the Main Group Elements*; Academic Press: New York, 1975; Chapter 3, pp 68–78. Boocock, S. K.; Shore, S. B. In *Comprehensive Organometallic Chemistry*; Wilkinson, G., Stone, F. G. A., Abel, E. W., Eds.; Pergamon Press: Oxford, England, 1982; Vol. 6, Chapter 41.2, pp 847–981. Whitmire, K. H. *J. Coord. Chem., Sect. B* **1988**, *17*, 95–111. Compton, N. A.; Errington, R. J.; Norman, N. C. *Adv. Organomet. Chem.* **1990**, *31*, 91–108.

(27) Forder, R. A.; Green, M. L. H.; McKenzie, R.; Poland, J. S.; Pront, K. *J. Chem. Soc., Chem. Commun.* **1973**, 426–427.

(28) Rettig, S. J.; Storr, A.; Thomas, B. S.; Trotter, J. *Acta Crystallogr.* **1974**, *B30*, 666–672. Forder, R. A.; Prout, K. *Acta Crystallogr.* **1974**, *B30*, 2312–2317.

(29) Corradini, P.; Sirign, A. *Inorg. Chem.* **1967**, *6*, 601–605.

(30) Fryzuk, M. D.; Huang, L.; McManus, N. T.; Paglia, P.; Rettig, S. J.; White, G. S. *Organometallics* **1992**, *11*, 2979–2990.

(31) Pörschke, K.-R.; Kleimann, W.; Tsay, Y.-H.; Krüger, C.; Wilke, G. *Chem. Ber.* **1990**, *123*, 1267–1273.

(32) de Miguel, A. V.; Gómez, M.; Isobe, K.; Taylor, B. F.; Mann, B. E.; Maitlis, P. M. *Organometallics* **1983**, *2*, 1724–1730.

(33) Mayer, J. M.; Calabrese, J. C. *Organometallics* **1985**, *3*, 1292–1298.

(34) Beletskaya, I. P.; Voskoboynikov, A. Z.; Chuklanova, E. B.; Kirillova, N. I.; Shestakova, A. K.; Parshina, I. N.; Gusev, A. I.; Magomedov, G. K.-I. *J. Am. Chem. Soc.* **1993**, *115*, 3156–3166 and references cited therein.

(35) Bursten, B. E.; Gatter, M. G. *J. Am. Chem. Soc.* **1984**, *106*, 2554–2558.

(36) Patmore, D. J.; Graham, W. A. *Inorg. Chem.* **1967**, *6*, 981–988. Fischer, R. A.; Miehr, A. Unpublished results, 1993–1994. Miehr, A. Diploma Thesis, Technical University of Munich, 1994.

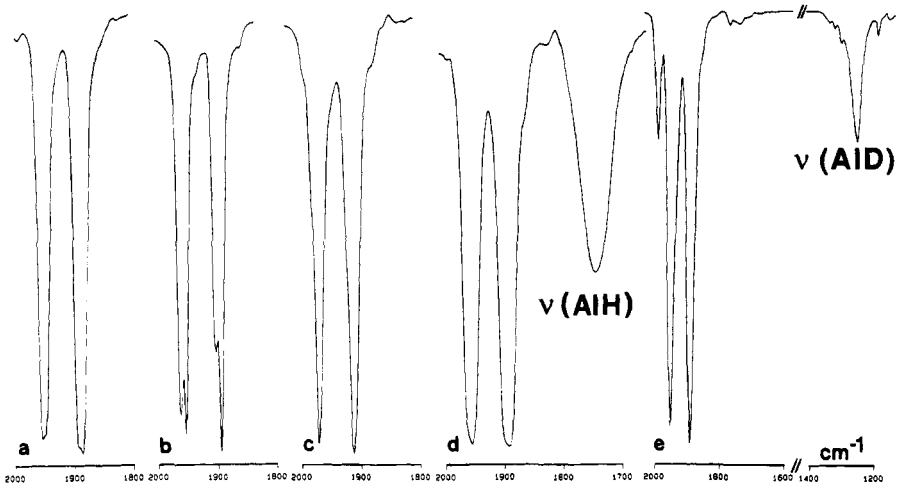

Figure 1. Solution infrared spectra in the carbonyl region (2000–1800 cm^{-1}) obtained in CaF_2 cells (toluene, 25 °C): (a) **2a** (c = 0.5 mol/L); (b) **2a** (c = 0.01 mol/L); (c) **2k**; (d) **2l** (extended range 2000–1700 cm^{-1}, including $\nu(Al-H_t)$ region); (e) D_2-**2l** (extended range 2000–1200 cm^{-1}, including $\nu(Al-D_t)$ region).

treated stepwise with organolithium reagents to obtain **2b**; this sequence substantiates the synthetic potential of compounds similar to **2k** (Scheme 1). The existence of **2l,m**, which exhibit AlH_2 moieties in the coordination sphere of a transition-metal fragment, is also quite remarkable, especially in light of the rather fruitless search for analogous compounds of the lighter homolog boron.[37] During the synthesis of **2k,m** the donor ligand NMe_3, which was present in the starting aluminum compounds **1e,g**, was substituted by a THF molecule from the solvent. In the case of the related gallium chemistry the NMe_3 base ligand does efficiently compete even with a large excess of THF and is retained in the final products. This reflects the differently balanced affinities of aluminum and gallium centers toward O and N Lewis bases in such compounds.

Previous attempts by other groups to obtain transition-metal–aluminum bonds using aluminum halides and salt elimination reactions have apparently been unsuccessful.[38] Also, we cannot confirm the formation of $(\mu_3\text{-Al})[Co_3(CO)_9]$[39] from $AlCl_3$ and $Na[Co(CO)_4]$. The products obtained from this latter reaction contain isocarbonyl structure elements.[40] Reactions between aluminum halides and transition-metal carbonylates show an inverse salt effect. With cations such as $[R_4Z^+]$ (Z = N, P, As; R = alkyl, aryl) rather than alkali-metal cations (Na^+, K^+) as counterions for the transition-metal carbonylates, halide substitution did not take place (IR spectroscopy). Ion-pairing effects appear to play a crucial role in controlling the reactivity between aluminum halides and transition-metal carbonylates.[41]

B. Spectroscopic Characterization. The electron impact mass spectra (70 eV) of **2a–e** show the molecular peak with very low relative intensities (~1%) only. The cleavage of the intermetallic bond is the predominant fragmentation process. Similar observations were made for some related organogallium and organoindium compounds.[42] The molecules of **2a–h** exhibit an asymmetrically coordinated Al center. Consequently, all the protons of the metallacycle, the methyl groups at the nitrogen donor atom, and the carbonyl substituents at the iron centers were found to be magnetically inequivalent on the NMR time scale within the examined temperature range of −90 to +150 °C. However, some variations of the line shapes were observed, which can be attributed to dynamic effects and the conformational flexibility of the chelate ring. The diastereotopic nature of the two CO ligands in **2a–h** causes a splitting of the single CO resonance at 220(±2) ppm observed for **2k–m** into two narrow lines of equal intensity separated by about 0.5(±1) ppm for **2a–h**. This is also a direct proof of the persistance of the M–Al bond in solution. Fe–Al bond dissociation, for example, would produce either a symmetrical $[(\eta^5\text{-}C_5H_5)(CO)_2Fe]$ fragment with magnetically equivalent CO substituents or the isocarbonyl structure Al–OC–Fe–CO with very different CO resonances. The latter structure can also be ruled out by IR spectroscopy (see below). The organogallium analogs to **2a–h** show a less rigid coordination geometry at the group 13 center. In that case, depending on the substituents and the temperature, coalescence phenomena, e.g. that involving the $N-CH_3$ resonances, were observed in the respective NMR spectra.[24] The strength of the dative Al–N bond appears to be less sensitive toward variations of the substituents R at the $Al[(CH_2)_3NMe_2](R)$ fragment. The solution IR spectra of **2a–m** have been measured in various solvents (n-pentane, toluene, THF, methylene chloride) and reveal the typical patterns A′ + A″ (**2a–c,f,g,k–m**) and A_1 + E (**2d,e,h**) for the entirely undissociated species (Figure 1). For **2a,b**, however, the two expected ν(CO) bands are split by about 10(±4) cm^{-1} each. A similar effect was observed for the analogous Fe–Ga compounds[24] and for the related thorium and uranium complexes $(\eta^5\text{-}C_5H_5)(CO)_2Ru\text{–}An(X)(\eta^5\text{-}C_5H_5)_2$ (X = Cl, $\eta^5\text{-}C_5H_5$)[43] and was attributed to some conformers which were resolved on the IR time scale at 25 °C (Figure 1).

(37) Basil, J. D.; Aradi, A. A.; Bhattacharyya, N. P.; Rath, N. P.; Eigenbrot, C.; Fehlner, T. P. *Inorg. Chem.* **1990**, *29*, 1260–1270.
(38) Schollenberger, M.; Nuber, B.; Ziegler, M. L.; Hey-Hawkins, E. *J. Organomet. Chem.* **1993**, *460*, 55–66.
(39) Schwarzhans, K. E.; Steiger, H. *Angew. Chem.* **1972**, *84*, 587–588.
(40) Schneider, J. Personal communication, Max-Planck Institut für Kohlenforschung, Mülheim, Germany.
(41) Darensbourg, M. Y. *Prog. Inorg. Chem.* **1985**, *33*, 221–274.
(42) Fischer, R. A.; Behm, J. *J. Organomet. Chem.* **1992**, *429*, 275–286. Kronseder, C.; Schindler, T.; Berg, C.; Fischer, R. A.; Niedner-Schatteburg, G.; Bodybey, V. E. *J. Organomet. Chem.* **1994**, *475*, 247–256.
(43) Sternal, R. S.; Brock, C. P.; Marks, T. J. *J. Am. Chem. Soc.* **1985**, *107*, 8270. Sternal, R. S.; Marks, T. J. *Organometallics* **1987**, *6*, 2621–2623.

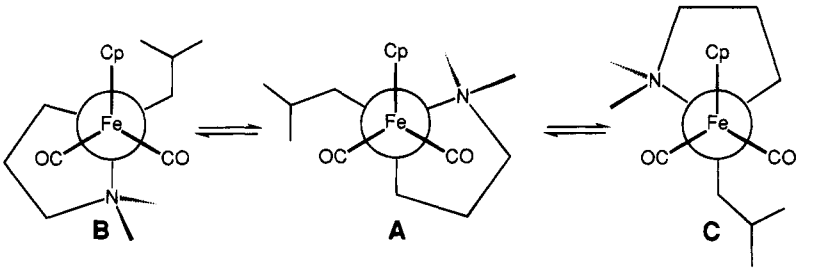

Figure 2. Schematic representation of different rotamers of compound **2a** (Newman projection along the Fe—Al axis). Structure **A** corresponds to the preferred orientation in the solid state (see Figure 3).

The shift to higher energy, $\Delta\nu(CO)^{as}$, of the asymmetric $^{12}C-O$ stretching vibration resulting from complex formation can be used as a measure of the acceptor strength of Lewis acids for the base $[(\eta^5\text{-}C_5H_5)(CO)_2Fe^-]$ ($\nu(CO)^{as}$ 1770 cm^{-1} [44]). In the present cases, $\Delta\nu(CO)^{as}$ values are typically around 120–140 cm^{-1}. For the related gallium compounds $(\eta^5\text{-}C_5H_5)(CO)_2Fe-Ga[(CH_2)_3NMe_2](R)$ (R = Cl, Et) $\Delta\nu(CO)^{as}$ equals 130–150 cm^{-1}, while for $[(\eta^5\text{-}C_5H_5)(CO)_2Fe-E(C_5H_6)_3]^-$ $\Delta\nu(CO)^{as}$ amounts to 90 cm^{-1} for E = Al, Ga but 139 cm^{-1} for E = B.[45] From this it may be concluded that the σ(Fe—Al) bonds of **2a–m** are still best described by a donor/acceptor model with a considerably large ionic contribution; however, they are clearly more covalent than in the negatively charged Lewis acid/base adduct mentioned above. Typically, covalent Fe—X bonds as in the alkyl systems $(\eta^5\text{-}C_5H_5)(CO)_2Fe-R$ exhibit $\Delta\nu(CO)^{as}$ around 170 cm^{-1}. In contrast to this, the respective values for $(\eta^5\text{-}C_5H_5)(CO)_2Fe-BR_2$ (R = C_6H_5, catecholate) are 180–200 cm^{-1}, attributed to significant Fe—B *multiple bonding*.[46] On the basis of this analysis it is interesting to note that the aforementioned Ru—Lu bond ($\nu(CO)^{as}$ 1965 cm^{-1}) appears to be substantially more covalent than its Ru—Al analogue **2g** ($\nu(CO)^{as}$ 1915 cm^{-1}). Another comparison can be made with actinide–transition-metal bonds of the type $(\eta^5\text{-}C_5H_5)(CO)_2M-An(X)(\eta^5\text{-}C_5H_5)_2$ (M = Fe, Ru; An = Th, U; X = Cl, CH_3, $\eta^5\text{-}C_5H_5$).[42] Depending on the substituent X, the $\nu(CO)^{as}$ values can be as low as 1873 cm^{-1} due to much more polarized M—An bonds. From this point of view the polarity of the M—Al bonds in **2a–m** is also very similar to the recently obtained new heterodinuclear "early–late" transition-metal compounds of the type $[H_3CC(CH_2NSiMe_3)_3]Ti-Fe(CO)_2(\eta^5\text{-}C_5H_5)$[47] and $(\eta^5\text{-}C_5H_5)(RN)M-Fe(CO)_2(\eta^5\text{-}C_5H_5)$[48] ($\Delta\nu(CO)^{as}$ ~146(±5) cm^{-1}). The ^{27}Al NMR resonances of **2a–m** were observed within the range 180–215 ppm (except **2k**, 156 ppm), at the low-field end of the usual range of four-coordinated organoaluminum compounds.[49] In comparison with the ^{27}Al NMR resonances for $X_2Al[(CH_2)_3NMe_3]_2$ (X = Cl, Br), arising around 140 ppm, it can be concluded that the Al center in the heterobimetallic compounds **2a–m** is significantly more deshielded. This also agrees well with a rather polar description of the Fe—Al bond.

The treatment of the quinuclidine-stabilized monobromoalane $H_2BrAl(NC_7H_{13})$ (**1f**) with the iron nucleophile $[Cp(CO)_2Fe]K$ according to Scheme 1 gave a yellow toluene-soluble and extremely air-sensitive, pyrophoric, microcrystalline product, which was analyzed correctly as $C_{14}H_{20}AlFeNO_2$. Unfortunately, no single crystals suitable for X-ray diffraction studies have been obtained so far. The IR spectra in solution (Figure 1) revealed the expected two $\nu(CO)$ absorptions of equal intensity and a broad band at 1748 cm^{-1}, which was assigned to terminal $\nu(Al-H_t)$ vibrations by deuteration experiments: $\nu(Al-D)$ = 1264(±4) cm^{-1} (calculated 1258 cm^{-1}). The Al—H ^1H NMR resonances were extremely broadened and were very difficult to assign. In the case of the related system **2m**, however, the Al—H resonances could be identified at δ 4.31 ppm, which disappeared upon deuteration (for comparison: $H_3AlNC_7H_{13}$ δ(Al—H) 3.87 ppm; for M—H—Al bridging hydrogen units, e.g. Ni—H—Al, −4.30 to −5.62 ppm[30]). The ^{27}Al NMR resonances for **2l,m** were observed at 220 ppm, which refer to a Fe—Al structure element by the comparison with compounds **2a–k**. Other possible aluminum species, e.g. $H_2XAl(NC_7H_{13})$ (X = H, Br, OR, etc.), show their ^{27}Al NMR resonances very much upfield below 140 ppm and were not detected in the spectra. The position of the carbonyl resonance at 221 ppm for **2l** is close to the values of 219 ppm observed for **2a–k**. By all these arguments it may be concluded that the principal structural features of compounds **2l,m** are very much similar to those of the related systems **2a–h**. In other words, **2l,m** contain terminal AlH_2 units which do not interact with the carbonyl substituents, giving Al—OC(H) moieties, or with the iron center, forming Fe—H—Al bridging units, which one could have expected.

C. Structure of Compound 2a. Structural data on transition-metal–aluminum bonds typically concern polynuclear cluster compounds, and there are very few other examples, which have already been mentioned earlier in the text. Dinuclear systems such as **2a–m**, which exhibit an organoaluminum moiety linked to a transition-metal fragment by a *nonbridged* metal–metal bond, are extremely rare. The presence of a σ-(Fe—Al) bond for **2a** was confirmed by an X-ray single-crystal structure analysis (Tables 2 and 3, Figure 3). The Fe—Al bond length of 2.456(1) Å compares to the significantly longer distance of 2.510(2) Å which was observed the Lewis acid/base adduct $[(\eta^5\text{-}C_5H_5)(CO)_2Fe-Al(C_5H_6)_3]^-$ mentioned above.[45] These values lie within the range of Fe—Al contacts of 2.30–2.80 Å found in intermetallic alloys such as $FeAl_3$[50] with an average bond length of 2.55 Å. Using accepted covalent radii for both metals, a value of 2.42 Å is estimated for a

(44) Nitay, M.; Rosenblum, M. *J. Organomet. Chem.* **1977**, *136*, C23–C25.
(45) Burlitch, J. M.; Leonowicz, M. E.; Petersen, R. B.; Hughes, R. E. *Inorg. Chem.* **1978**, *18*, 1097–1105.
(46) Hartwig, J. F.; Huber, S. *J. Am. Chem. Soc.* **1993**, *115*, 4908–4909.
(47) Friedrich, S.; Memmler, H.; Gade, L. H.; Li, W.-S.; McPartlin, M. *Angew. Chem., Int. Ed. Engl.* **1994**, *33*, 705–708.
(48) Sundermeier, J.; Runge, D. *Angew. Chem., Int. Ed. Engl.* **1994**, *33*, 1258–1261.
(49) Benn, R.; Janssen, E.; Lehmkuhl, H.; Rufinska, A. *J. Organomet. Chem.* **1987**, *333*, 155–168.
(50) Black, P. J. *Acta Crystallogr.* **1955**, *8*, 175–177.

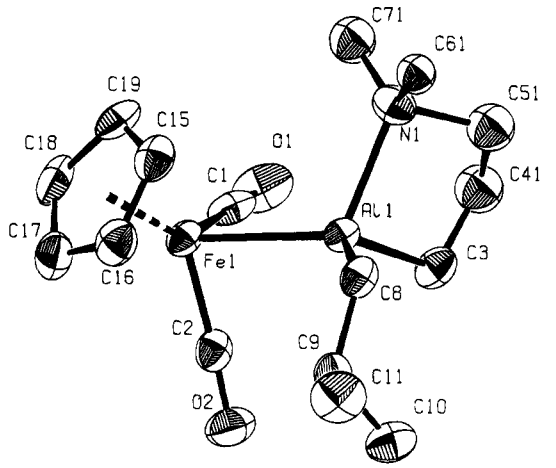

Figure 3. View of the molecular structure of **2a** in the solid state (ORTEP drawing; non-hydrogen atoms are shown as 50% thermal ellipsoids and hydrogen atoms are omitted). The atoms in the five-membered heterocycle (Al1, ..., N1) are disordered. For clarity, only one of the two different refined positions is shown in each case.

single bond. It is interesting to note that for the related compound (η^5-C_5H_5)$(CO)_2$Fe—Ga[$(CH_2)_3NMe_2$](Et) an Fe—Ga distance of 2.456(1) Å was found,[25] which is equal to the Fe—Al distance of **2a** within the accuracy of the measurement. However, this is not really surprising. First, the ionic and covalent bonding radii of Al and Ga do not differ much,[51] and second, metal—metal bonding potentials are usually quite shallow and thus rather sensitive toward steric effects.

The geometric parameters of the coordination sphere around the iron centers of **2a** and [(η^5-C_5H_5)$(CO)_2$Fe—Al-$(C_5H_6)_3$]$^-$ are very similar. In both systems the angle between the Fe—Cp vector and the plane defined by C1, Fe, and C2 are close to 160° and do not deviate much from the ideal value of 180° for the isolated anion [(η^5-C_5H_5)$(CO)_2$Fe]$^-$. Consequently, the angles OC—Fe—Al are quite small, roughly 82°, which is typical for rather negatively charged iron centers in (η^5-C_5H_5)$(CO)_2$-$Fe^{\delta-}X^{\delta+}$ compounds.[52] The angle C1—Fe—C2 of 92.5-(2)° in **2a** in the solid state is almost similar to the solution value of 94(2)° obtained from analyzing the IR ν(CO) intensities. The intramolecular contacts Al—O1 and Al—O2 of 3.50(±5) Å are clearly nonbonding. The aluminum atom rests in the center of a distorted-tetrahedral coordination sphere. This is mostly due to the rather small angle N—Al—C3 of 88.2(2)°, which is a consequence of the intramolecular Al—N adduct formation to give a five-membered metallacycle. Its envelope conformation is not very rigid, even in the solid state. In fact, the ring atoms C4 and C5 and the methyl substituents C6 and C7 are disordered. This is a common feature of intramolecular chelate structures involving the 3-(dimethylamino)propyl group.[24] The Al—N distance of 2.094(3) Å is in the usual range for dative bonds between nitrogen and four-coordinated aluminum.[2] The preferred staggered arrangement along the Fe—Al axis in the solid state is depicted as structure A in Figure 2. The deviation of the torsion angle

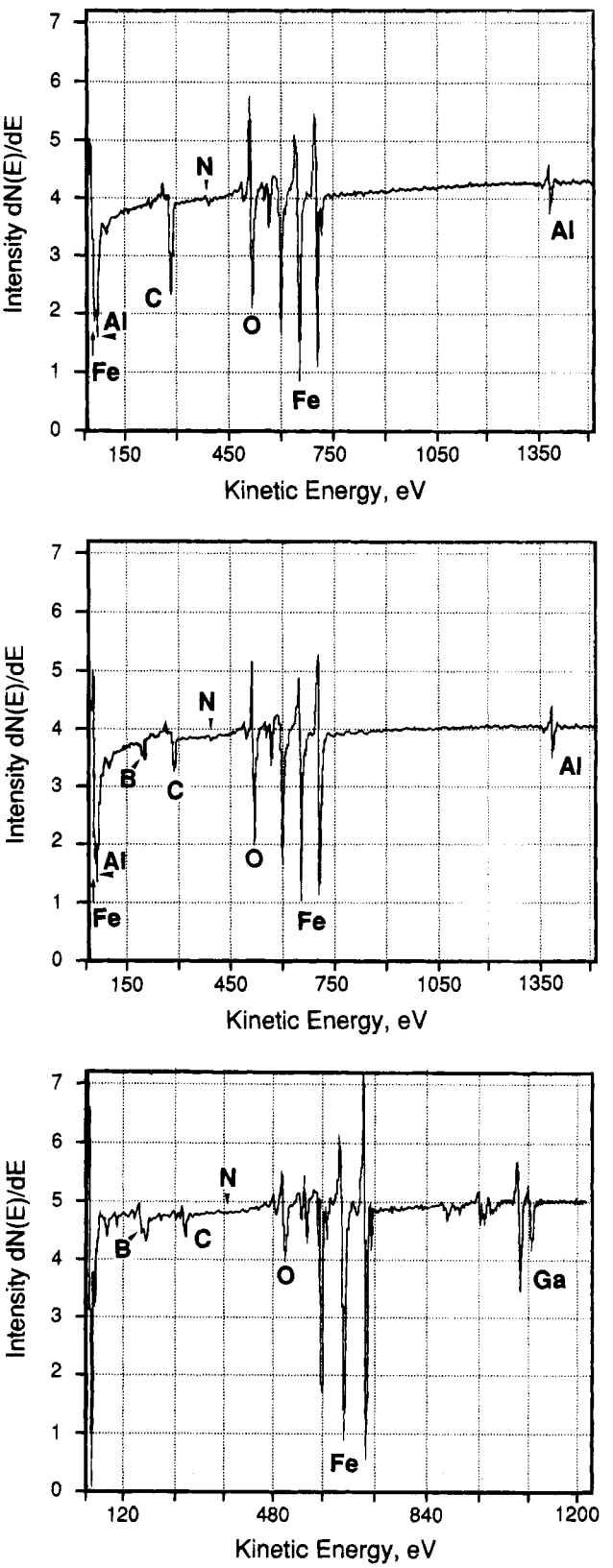

Figure 4. Auger spectra: (a, top) Fe/Al thin film grown from **2a** (Fe, 43(1); Al, 22(1); C, 19(1); O, 16(1)); (b, middle) Fe/Al thin film grown from **2c** (Fe, 42(1); Al, 32(1); C, 6(1); O, 15(1); B, 5(1)); (c, bottom) Fe/Ga thin film grown from (η^5-C_5H_5)$(CO)_2$Fe—Ga[$(CH_2)_3NMe_2$](BH_4) (**2c-Ga**) (Fe, 48-(1); Ga, 38(1); C, 3(1), O, 4(1)[25]) Conditions: Perkin-Elmer Phi 595, 3 kV, 0.2 μA primary beam intensity; 2 min of Ar ion sputtering to remove surface impurities; thin film compositions (atom %) estimated to be correct within a relative error of 10—20%.

(51) Ionic radii (Å) for E^{3+} (coordination number 4): 0.53 (Al), 0.61 (Ga) (Shannon, R. D. *Acta Crystallogr.* **1976**, *A32*, 751). Covalent bond radii (Å) for R_2E units (R = alkyl, aryl): 1.33 (Al), 1.25 (Ga). Radii derived as half of the E—E distances in the compounds R_2E—ER_2 (R = 2,4,6-*i*-$Pr_3C_6H_2$): 1.32 (Al), 1.25 (Ga) (Wehmschulte, R. J.; Ruhland-Senge, K.; Olmstead, M. M.; Hope, H.; Sturgeon, B. E.; Power, P. P. *Inorg. Chem.* **1993**, *32*, 2983—2984).

(52) Fischer, R. A.; Herdtweck, E.; Priermeier, T. *Inorg. Chem.* **1994**, *33*, 934—943 and references cited therein.

Scheme 2

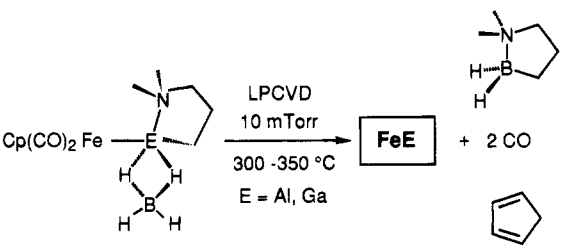

C2—Fe—Al—N of 161.6(2)° from its "ideal" value of 180° is due to the small angle C3—Al—N. An analysis of the variation of the intramolecular nonbonding contacts, upon torsion around the Fe—Al axis, show that the minimization of steric interactions between the N—CH_3 groups and the CO substituents may control the conformation of the molecule in the solid state. In the related transition-metal gallium and indium chemistry similar observations were made when the 3-(dimethylamino)propyl group was involved.[25,52] From these analyses one may conclude that the rotation along the σ(Fe—Al) bond of **2a** is not completely free due to steric interactions. In conclusion, the structural features of **2a** in the solid state are in full agreement with its structure in solution.

D. OMCVD Experiments. Some low-pressure MOCVD experiments using a horizontal hot-walled tube reactor were carried out with the Fe—Al and Co—Al compounds **2a—d**. At substrate temperatures above 350 °C adherent, reflective, amorphous (XRD) intermetallic thin films MAl_{1-x} (M = Fe, Co; x = 0.1—0.5; by AAS) with thicknesses of ~2000 Å were deposited (rates up to 1 μm/h). The Fe—Al compound **2a** proved to be surprisingly thermally stable. Below 350 °C most (>90%) of the precursor **2a** passed through the hot zone and was collected unchanged in the cold trap. The films were significantly contaminated with carbon and oxygen (best values 5—15 atom % C and O by Auger spectroscopy) but were essentially free of N (Figure 4). The resistivities were thus rather high, >500 μΩ·cm (four-point probe). This is in contrast to our earlier results on transition-metal gallium and indium thin films which had been grown under the same conditions from related transition-metal gallium and indium precursors. Those intermetallic deposits, e.g. β-CoGa and ε-NiIn, were single-phased and crystalline and were much purer, with C, O, and N levels at the AES detection limit of 1 atom %.[8] The introduction of the tetrahydroborato group in **2c** gave some improvement in reducing both the deposition temperature (~300 °C for 100% decomposition) and the level of impurities (C, O ~5 atom %). Because we could not succeed in synthesizing pure **2c**, the obtained mixture of **2c** and **2f** (see section A) was used in these experiments. At the moment we are thus unable to establish an exact mass balance for the deposition of Fe/Al thin films from **2c**. In the related Fe/Ga case, however, where pure (η^5-C_5H_5)$(CO)_2$Fe—Ga-[$(CH_2)_3NMe_2$](BH_4) (**2c-Ga**) was available as precursor,[25] the effect of the BH_4 substituent could be analyzed much better and is apparently due to the reaction process sketched in Scheme 2,[25] which may also be true for the Fe/Al case.

The exhaust gases, which usually consist of unsaturated hydrocarbons (e.g. for **2a—d**: H_2C=$CHMe_2$, PMe_3, *cyclo*-C_5H_6, H_2C=$CHCH_2NMe_2$, and various isomers of this), contained a large amount (~40—50% by GC/MS) of the alkylborane $H_2B[(CH_2)_3NMe_2]$ (identified also by NMR). The species $\{HB[(CH_2)_3NMe_2]^+\}$ ($m/_z$ 98; for ^{11}B)[53] was detected in the high-resolution electron impact mass spectra of both the pure compound **2c-Ga** and the **2c/2f** mixture. These species were also detected by in situ mass spectroscopy of the exhaust gases at the end of the reactor. With **2c-Ga** as precursor, the exhaust gases only contained traces of iron compounds (AAS of the condensables after aqueous workup). With the mixture of **2c/2f** as precursor, only **2f** passed the hot zone and collected unchanged in the cold trap behind. In an independent experiment it was shown that compound **2f** does not significantly pyrolyze below 500 °C(!).

From this preliminary screening of the compounds **2a—d** it appears that it is much more difficult to obtain pure M/Al thin films from transition-metal carbonylate organoaluminum precursors than M/E thin films (E = Ga, In) from related gallium and indium congeners (Figure 4). This can be attributed to the higher Al—C and Al—N bond strengths and the stronger affinity of the aluminum centers toward the carbonyl oxygen atoms, which may be important during the decomposition process. Further experiments are in progress and will be presented elsewhere.

E. Conclusions. Lewis base adduct formation at the aluminum center is an attractive concept to stabilize R_2Al (R = H, halide, alkyl) moieties in the coordination sphere of transition-metal carbonylate fragments. In those compounds the known tendency of the Al center to attack carbonyl ligands to give M—CO—Al isocarbonyl coordination or to transfer R groups is significantly suppressed. The new nonbridged σ(M—Al) interactions are rather polar. The stability of those bonds is controlled by the donor/acceptor properties and the steric requirements at the two metal centers. With a halide substituent and intramolecular adduct formation at the Al center thermally very robust derivatives can be obtained, e.g. compound **2f**. The potential of the new compounds to serve as single-source precursors to deposit intermetallic aluminides M/E by MOCVD techniques warrants further investigation.

Acknowledgment. This work was supported by the "Deutsche Forschungsgemeinschaft" (Grant No. Fi 502/2-1 and 2-2), the "Fonds der Chemischen Industrie", and the "Leonhardt-Lorenz Foundation" of the Technical University of Munich.

Supplementary Material Available: Tables of atom coordinates and isotropic thermal parameters, bond distances and angles, hydrogen coordinates, and anisotropic thermal parameters (8 pages). Ordering information is given on any current masthead page.

OM940309P

(53) Kronseder, C. Diploma Thesis, Technical University of Munich, 1993.